PHYSICAL REVIEW A VOLUME 26, NUMBER 1 JULY 1982

Quantum theory of atom-ellipsoid scattering in two dimensions

S. Bosanac,
R. Bošković Institute, 41001 Zagreb, Croatia, Yugoslavia
(Received 12 May 1981)

The theory of atom-ellipsoid scattering in two dimensions is developed. The model is typical of atom-molecule rotationally inelastic collisions. It is shown that the problem is not suitable for the use of the standard techniques because of the presence of the hard core in the potential and the semiclassical character of the system. In this article several points are discussed: the choice of the proper technique for solving the problem, the convergence problem of the perturbation schemes for the coupled multichannel equations, forbidden transitions and features of the cross sections, and finally, the static limit of the equations.

I. INTRODUCTION

Recent results of using a simple model or atom-molecule scattering have contributed to our understanding of the rotational collision process.[1,2] In such a model the molecule is replaced by a rigid ellipsoid in which case the classical equations of motion can be solved exactly. By simplifying the model even further, i.e., treating only the two-dimensional problem, it is shown that very useful expressions can be derived, relating the features of the inelastic cross sections of the parameters characterizing the ellipsoid.[1] Use of this formula for interpreting the experimental results has shown that such a model is valuable for analyzing the cross sections in terms of the features of the potential surface.[3] Although such a model may not be of use in all cases,[4] it stresses the need for properly taking into account the topological properties of the surface. Just for the sake of comparison, we can mention the usual procedure in the theory of inelastic collisions. The potential surface, for homonuclear molecules, is given as an expansion:

$$V(r,\theta)=V_0(r)+V_2(r)P_2(\hat{l}\hat{j}) + V_4(r)P_4(\hat{l}\hat{j})+\cdots , \tag{1.1}$$

where $\hat{l}$ and $\hat{j}$ are the unit vectors of the orbital and rotational angular momentum, respectively. Such an expansion implicitly assumes the spherical topology of the target, i.e., the target is essentially a sphere with the slight deviations, contained in the terms with the Legendre polynomials. Now this is not true (except few cases) and as we will show in Sec. II, the expansion (1.1) contains hidden dangers.

To a great extent, the purpose of this paper is to show explicitly why the topology of the system should be correctly taken into account and how this can be achieved. As an example we will try to solve and analyze the two-dimensional scattering of a particle on the ellipsoid, but the procedure is more general, and even applies to three dimensions with the relevant modifications. The basic conclusion is that once the topology of the system is taken into account the other features of the potential surface, which are not due to the hard core, can be treated as a perturbation.

Besides this problem, we would also like to give a method for calculating the cross sections. Although the model is restricted to only two dimensions, so that the absolute magnitude of the cross sections will not be given correctly, there are certain features which can be used for comparison with experiment. For example, the classical two-dimensional model[1] predicts oscillations in the differential cross sections. These oscillations are the result of the intereference between two waves scattered from the two orientations of the ellipsoid (see Ref. 1 where this point is discussed and also Secs. VI and VII of this paper). The spacing of these oscillations carries the information about the topology of the system, and the oscillations are essentially unaffected by doing the proper three-dimensional calculations.[5]

Working only in two dimensions greatly reduces the mathematical difficulties. Therefore, we are able to set up and analyze the equations in a more explicit way. In some cases, e.g., the static limit, we are even able to find the analytic solution of our problem (see Sec. VIII). Much of the paper is devoted to the discussion of different approximate

schemes which also bears relevance to the three-dimensional case, and also to the case of potentials which are realistic, i.e., not hard-core types but with some structure. In particular, we discuss the weak-coupling limit and the static approximation, which is a generalized analog of the sudden approximation.[6]

II. DEFINING THE PROBLEM

The Schrödinger equation for a system of a particle and a hard-core ellipsoid, in two dimensions, is

$$\left[\frac{\partial^2}{\partial r^2}+\frac{1}{r^2}\frac{\partial^2}{\partial\theta^2}+\frac{\mu}{I}\frac{\partial^2}{\partial\phi^2}\right]\psi=(V-k^2)\psi\ , \tag{2.1}$$

where μ is the reduced mass of the system and I is the momentum of inertia of the ellipsoid. The relevant coordinates are shown in Fig. 1. The potential is either infinite or zero, depending on the value of r and angle $\alpha=\theta-\phi$, and this relationship is determined from the boundary of the ellipse. In order to have the angle α explicitly in the kinetic energy, let us transform (2.1) into

$$\left[\frac{\partial^2}{\partial r^2}+\frac{1}{r^2}\left[\frac{\partial^2}{\partial\theta^2}+\frac{\partial^2}{\partial\alpha^2}\right]+\epsilon\frac{\partial^2}{\partial\alpha^2}+\frac{2}{r^2}\frac{\partial^2}{\partial\theta\partial\alpha}\right]\psi =[V(r,\alpha)-k^2]\psi\ , \tag{2.2}$$

where from now on we will designate $\epsilon=\mu/I$.

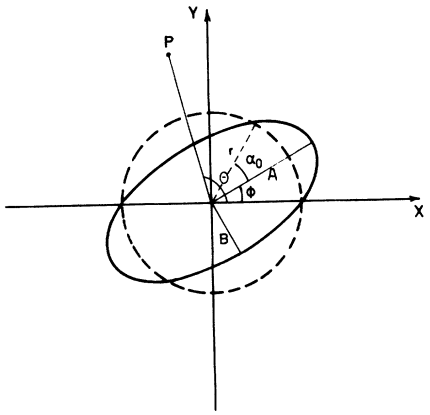

FIG. 1. Geometry of the system particle-ellipsoid in two dimensions. The particle P is coming parallel to the x axis and approaching the ellipsoid from the left. If particle P is at the distance $r>A$ from the center of ellipse it will not observe the presence of the hard-core potential. For $B<r<A$ the particle will hit the hard core at the intersection of the broken circle with the ellipse.

As the first attempt to solve (2.2) we can expand the solution ψ in the partial waves, and for two dimensions this is

$$\psi=\sum_{J,j}e^{iJ\theta+ij\alpha}\varphi_{J,j}(r)\ . \tag{2.3}$$

By replacing ψ in (2.2) with (2.3) we obtain a set of equations

$$\frac{d^2}{dr^2}\varphi_{J,j}=\left[\frac{(J+j)^2}{r^2}+\epsilon j^2-k^2\right]\varphi_{J,j} +\sum_{J',j'}V_{J,jiJ',j'}(r)\varphi_{J',j'}\ . \tag{2.4}$$

It is easy to show that the matrix elements $V_{J,j;J',j'}$ are exactly zero for $r>A$. However, for $B<r<A$ the integration path α in

$$V_{J,j;J',j'}(r)=\frac{\delta_{J,J'}}{2\pi}\int_0^{2\pi}V(r,\alpha)e^{i\alpha(j'-j')}d\alpha \tag{2.5}$$

goes partly through the region where V is infinite and partly through the region where it is zero. The integration path is shown in Fig. 1 by the broken line. Therefore, (2.5) is, in general, infinite, which also means that solving the problem of inelastic particle-ellipsoid scattering runs into the difficulties if we use the cylindrical coordinates. This is reflected in the fact that we have to solve a system of coupled differential equations for which the coupling matrix is infinite. In reality, the potential is not the hard-core ellipsoid, but even so the largest contribution to the matrix elements (2.5) comes from the nonphysical, repulsive region of the potential. As we have just shown, these problems are artificial, arising primarily from the use of the wrong method of expansion for ψ. Therefore, we must use an alternative procedure to replace simple partial-wave decomposition (2.3).

Before suggesting alternatives, let us look again at (2.5). We assume that the potential inside the ellipsoid is not infinite but has some large value V_0. In that case, we can find the matrix elements (2.5), and they are given by

$$V_{J,j;J',j'}=\frac{V_0}{\pi}\delta_{J,J'}\frac{\sin\alpha_0(j'-j)}{j'-j}[1+(-1)^{j'+j}]\ , \tag{2.6}$$

where α_0 is defined as the angle between the large axis A and the point of intersection between the circle of the radius r and the ellipse (see Fig. 1). It

is easily shown that α_0 is a function of r. As we have argued earlier, and from (2.6) explicitly, the coupling matrix elements contain the part which describes the nature of the scatterer [this is given by the functional relationship $\alpha_0(r)$], but everything is scaled by an arbitrary large factor V_0. This nonphysical factor is present, but not explicitly evident, if one uses the expansion (1.1) for the potential and single eigenfunctions of the rigid rotor.

One alternative is to use noncylindrical coordinates. Since the problem is always averaging the potential over the one or several coordinates, the new coordinates must be defined in such a way that the equivalent of the radial coordinate is constant on the surface of the scatterer. In our example this is the elliptical coordinate system.[7] It can be shown that, concerning the potential, the problem is now equivalent to the scattering of two hard-core spheres with all the coupling in the kinetic energy. As a result of using the noncylindrical coordinates, the problem becomes more complicated but the nature of the difficulties is of a different sort. We do not get the infinite coupling matrix; instead, the kinetic energy is complicated but finite.

In order to preserve the simplicity of the kinetic energy obtained with cylindrical coordinates, in this article we will try another way to solve the problem. We will combine the simplicity of the cylindrical coordinates and at the same time take into account the fact the wave function inside the ellipse is exactly zero. To achieve this, let us notice that in evaluating (2.6) the difficulty was in the use of the functions $e^{ij\alpha}$ which did not distinguish between the region of infinite and zero potential. Let us, therefore, plot the potential; $V(r,\alpha)$, as the particle, would "see" it when going through the full circle of 2π. We find the square wells with the infinite walls, as shown in Fig. 2.

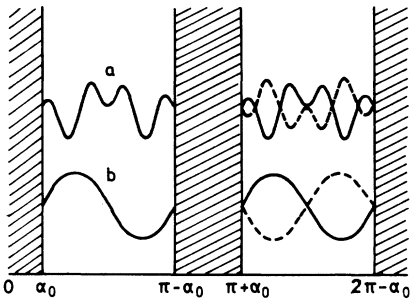

FIG. 2. Plot of the particle-ellipsoid potential for a fixed r and variable angle α. For a definition of the angles α and α_0 see Fig. 1. The standing waves χ_2^0 (line a) and χ_2 (line b) are formed in the potential wells, which replace the angular eigenfunctions of the rigid rotor.

For such a potential we can solve the eigenvalue problem of the angular part of the Schrödinger equation (2.2), i.e., we have to solve the equation

$$\left[\frac{1}{r^2}\left[\frac{\partial^2}{\partial\theta^2}+\frac{\partial^2}{\partial\alpha^2}\right]+\epsilon\frac{\partial^2}{\partial\alpha^2}+\frac{2}{r^2}\frac{\partial^2}{\partial\theta\partial\alpha}\right]\chi_m^J = (V-\lambda_m)\chi_m^J \tag{2.7}$$

subjected to the periodicity condition that χ_m^J is invariant to translation $\alpha\rightarrow\alpha+2\pi$. We also impose the condition that at points $\alpha=\alpha_0$, $\pi-\alpha_0$, $\pi+\alpha_0$, and $2\pi-\alpha_0$, the eigenfunction χ_m^J is zero. The normalized solution of (2.7), with such properties, is

$$\chi_m^{\pm}=\frac{1}{\sqrt{\pi-2\alpha_0}}\left[e^{ia\alpha}\sin\left[\frac{m\pi}{\pi-2\alpha_0}(\alpha-\alpha_0)\right]\right]\oplus(\alpha\rightarrow\alpha-\pi),\quad m\geq 1 \tag{2.8}$$

where $a=-J/(1+\epsilon r^2)$. The symbol $\oplus$ means that the term inside the square bracket is repeated in the interval $\pi+\alpha_0<\alpha<2\pi-\alpha_0$. Another solution of (2.7) is the same as (2.8) in the interval $\alpha_0<\alpha<\pi-\alpha_0$ but opposite in the sign in the interval $\pi+\alpha_0<\alpha<2\pi-\alpha_0$. This solution of (2.7) is designated $\chi_m^{J^-}$.

Since the factor $\exp(iJ\theta)$ in (2.8) is well known for the total angular momentum, we will not write it from now on so that (2.8) is simplified:

$$\chi_m^{\pm}=\frac{1}{\sqrt{\pi-2\alpha_0}}\left[e^{ia\alpha}\sin\left[\frac{m\pi}{\pi-2\alpha_0}(\alpha-\alpha_0)\right]\right]\oplus(\alpha\rightarrow\alpha-\pi)\,. \tag{2.9}$$

For $m=2$ the functions (2.9) are shown in Fig. 2. The corresponding eigenvalues in (2.7) are

$$\lambda_m=\frac{\epsilon J^2}{l+\epsilon r^2}+\frac{1+\epsilon r^2}{r^2}\frac{m^2\pi^2}{(\pi-2\alpha_0)^2},\quad m\geq 1\,. \tag{2.10}$$

The functions (2.9) form a complete set, therefore we can write ψ in the form

$$\psi=\frac{1}{\sqrt{2\pi}}\sum_{J_p^m} e^{iJ\theta}\chi_m^p\varphi_{J,m}^p \ , \tag{2.11}$$

where p stands for parity. However, χ_m^p is now a function of two variables: α and r. Therefore (2.11) is not equivalent to (2.3) but resembles the Born-Oppenheimer expansion.[8] Hence, by avoiding the difficulty in using $e^{ij\alpha}$ as an expansion set, we had to introduce a set of angular eigenfunctions which were r dependent.

Another useful basis, which will be used in Sec. III, is defined as the eigenvectors of the operator $d^2/d\alpha^2$ subjected to the same boundary conditions as the solutions (2.9). This set is given by

$$\chi_m^{0\pm}=\frac{1}{\sqrt{\pi-2\alpha_0}}\left[\sin\left[\frac{m\pi}{\pi-2\alpha_0}(\alpha-\alpha_0)\right]\right]\oplus(\alpha\rightarrow\alpha-\pi) \ , \tag{2.12}$$

and the corresponding eigenvalues are

$$\lambda_m^0=\frac{1+\epsilon r^2}{r^2}\frac{m^2\pi^2}{(\pi-2\alpha_0)^2} \ . \tag{2.13}$$

In Fig. 2. the curve b shows (2.12) for $m=2$.

We will need later the unitary transformation between the sets (2.12) and (2.9), i.e., a transformation matrix with the property

$$\chi=T\chi^0 \ . \tag{2.14}$$

It is straightforward to show that the matrix elements of T are

$$T_{m,n}=\frac{2a'}{\pi}e^{i(\pi/2)(a+m+n)}\left[\frac{1}{a'^2-(m-n)^2}-\frac{1}{a'^2-(m+n)^2}\right]\sin\left[\frac{\pi}{2}(a'+m+n)\right] \ , \tag{2.15}$$

where

$$a'=a\frac{\pi-2\alpha_0}{\pi}=-\frac{J}{1+\epsilon r}\frac{\pi-2\alpha_0}{\pi} \ . \tag{2.16}$$

III. NONLINEAR REPRESENTATION OF THE SCHRÖDINGER EQUATION

Replacing the expansion (2.11) in (2.2) we obtain a set of equations for $\varphi_{J,m}^p$. However, such a procedure becomes very complicated, therefore we will proceed in a different way. We will firstly transform (2.2) in the basis χ_0 given by (2.12). This is achieved by writing χ in the form of expansion

$$\psi=\frac{1}{\sqrt{2\pi}}\sum_{J,m}\chi_m^{0p}\varphi_{J,m}^p e^{iJ\theta} \ , \tag{3.1}$$

and if such ψ is replaced in (2.2) we obtain a set of equations for $\varphi_{J,m}^p$. Using the orthonormality property of the basis χ_0, we obtain

$$\varphi_m''-\frac{J^2}{r^2}\varphi_m-\lambda_m^0\varphi_m+\sum_{n\geq 1}\left[\varphi_n\int_0^{2\pi}\chi_m^0\chi_n^{0\prime\prime}d\alpha+2\varphi_n'\int_0^{2\pi}\chi_m^0\chi_n^{0\prime}d\alpha+\frac{2iJ}{r^2}\varphi_n\int_0^{2\pi}\chi_m^0\frac{\partial}{\partial\alpha}\chi_n^0 d\alpha\right]=-k^2\varphi_m \ , \tag{3.2}$$

where we have omitted the indices for parity (p) and the total angular momentum (J). The parity index will become important in the derivation of the scattering amplitude.

The integrals in (3.2) can be evaluated analytically provided the derivatives of χ_0 are calculated first. After some algebra we obtain for (3.2)

$$\varphi''-\frac{4\alpha_0'}{\pi-2\alpha_0}E\varphi'-\left[\frac{2\alpha_0'}{\pi-2\alpha_0}\right]'E\varphi+\left[\frac{2\alpha_0'}{\pi-2\alpha_0}E\right]^2\varphi-\frac{J^2}{r^2}\varphi-\lambda^0\varphi-\frac{4iJ}{r^2}\frac{1}{\pi-2\alpha_0}C\varphi=-k^2\varphi\ , \tag{3.3}$$

where we have used the matrix notation. The matrices E and C are

$$E_{m,n}=\begin{cases}\dfrac{mn}{m^2-n^2}[1+(-1)^{m+n}], & m\neq n\\ 0, & m=n\ ,\end{cases} \tag{3.4a}$$

$$C_{m,n}=\begin{cases}\dfrac{mn}{m^2-n^2}[(-1)^{m+n}-1], & m\neq n\\ 0, & m=n\ .\end{cases} \tag{3.4b}$$

The integration variable r in (3.3) is defined in the interval $B\leq r\leq A$ and for the limiting values of r the angle α_0 is $\alpha_0(B)=\pi/2$ and $\alpha_0(A)=0$. Some of the coefficients in (3.3) are therefore infinite in the limit $r\to B$, which imply the initial value $\varphi=0$ for $r=B$.

The set of equations (3.3) is relatively complicated and we can simplify it by defining a new function y:

$$y=T^+YT\ , \tag{3.5}$$

where

$$Y=\varphi\left[\varphi'-\frac{2\alpha_0'}{\pi-2\alpha_0}E\varphi\right]^{-1}\ . \tag{3.6}$$

The unitary matrix T is defined in (2.15) and φ is the regular solution of (3.3). There are several reasons for using the function (3.5) instead of φ and φ': (a) as will be shown in Sec. IV, the S matrix is directly given in terms of y, similarly as in the one-dimensional case.[9] Therefore it is more natural to work with y rather than with φ and φ' separately, (b) the function y satisfies a set of the first-order nonlinear equations, for which it can be proved that it is numerically stable for integration. Similar analysis shows that the set (3.3) is numerically unstable, with a very serious accumulation of error in the course of integration, (c) the function y is symmetric, thus reducing the number of equations for integration by almost a factor of 4, (d) the set of equations (3.3) is very difficult to analyze but the equivalent set for y is much simpler.

To obtain the set of equations for y we proceed as follows. We take derivative of Y in which case we obtain

$$Y'=I+\frac{2\alpha_0'}{\pi-2\alpha_0}(EY-YE)$$

$$-Y\left[\frac{J^2}{r^2}+\lambda^0+\frac{4iJ}{r^2}\frac{C}{\pi-2\alpha_0}-k^2\right]Y\ . \tag{3.7}$$

In the next step we take derivative of y and obtain

$$y'=I+\left[T^{+\prime}T+\frac{2\alpha_0'}{\pi-2\alpha_0}T^+ET\right]y$$

$$-y\left[\frac{2\alpha_0'}{\pi-2\alpha_0}T^+ET-T^+T'\right]-y(\lambda-k^2)y\ , \tag{3.8}$$

where λ is the eigenvalue matrix (2.10) which was obtained by transforming the angular part of the Hamiltonian, present in the bracket of (3.7), into the basis χ. The notation in (3.8) is simplified if we define a unitary matrix U by

$$U=\exp[E\ln(\pi-2\alpha_0)]T\ , \tag{3.9}$$

in which case (3.8) is

$$y'=I+yU^+U'-U^+U'y-y(\lambda-k^2)y\ . \tag{3.10}$$

In the Appendix we show how the product U^+U' is calculated, where we also designate it by η.

The set (3.10) is complex. We can make it real by defining a diagonal matrix V:

$$V=(I+iI^-)/\sqrt{2}\ , \tag{3.11}$$

where I is the unit matrix and I^- has ones for the odd indices and -1 for the even indices. The solution y can now be written as

$$y=(I-iI^-)y_R(I+iI^-)/2\ , \tag{3.12}$$

where y_R is now a real matrix. The set of equations for y_R is

$$y_R'=I+y_R\eta_R-\eta_Ry_R-y_R(\lambda-k^2)y_R\ , \tag{3.13}$$

where the real matrix η_R is defined in the Appendix. From now on the index R will be omitted because we will always refer to the set of equations (3.13), if not stated otherwise. The solution of (3.13) determines the S matrix for the atom-ellipsoid scattering, as is shown in Sec. IV.

IV. SCATTERING AMPLITUDE

Because of the special nature of our problem, using the basis set (2.9) and two dimensions, we will briefly outline the calculation of the scattering amplitude and the S matrix. By our assumption, the incident wave is coming along the x axis, from the negative to the positive values. Hence, far away from the scatterer we have

$$\psi_m \sim e^{ik_m x+im\phi}+\frac{1}{\sqrt{r}}\sum_{m'} e^{ik_{m'}r+im'\phi} f_{m',m}(\theta) \ . \quad (4.1)$$

Since the angle ϕ is not explicitly present in the calculations, but rather the angle $\alpha=\theta-\phi$, the scattering amplitude is given by

$$F_{m',m}(\theta)=e^{im'\theta} f_{m',m}(\theta) \ . \quad (4.2)$$

It should be noted that the range of the scattering angle is not $0°<\theta<180°$, as in the three dimensions, but is defined in the interval $0°<\theta<360°$.

Let us now replace the plane wave in (4.1) by[10]

$$e^{ikx}=\tfrac{1}{2}\sum_{l=-\infty}^{\infty} i^l[H_l^{(1)}(kr)+H_l^{(2)}(kr)]e^{il\theta} \ , \quad (4.3)$$

where $H_k^{(j)}(z)$, $j=1,2$, are the Hankel functions. We also write (4.2) in a partial-wave series

$$F_{m',m}(\theta)=\sum_{J=-\infty}^{\infty} e^{iJ\theta}F^J_{m',m} \ , \quad (4.4)$$

where $F^J_{m',m}$ are the partial-wave amplitudes.

The S matrix $S^J_{m,m'}$ is now defined in an analogy to the three-dimensional case

$$F^J_{m',m}=\frac{e^{-i(\pi/4)}}{(2\pi k_{m'})^{1/2}}(S^J_{m',m}-\delta m,m') \ . \quad (4.5)$$

Since outside the ellipse, i.e., for $r>A$, the potential is everywhere zero, the spherical waves in (4.1) are the asymptotic limits of the free-particle solution, therefore we replace e^{ikr} by

$$\frac{1}{r}e^{ikr}\rightarrow\left[\frac{\pi k}{2}\right]^{1/2} e^{i(\pi/2)(l+1/2)}H_l^{(1)}(kr) \ . \quad (4.6)$$

We have now all the essential quantities for the right side of (4.1). To obtain now $S^J_{m,m'}$, or the scattering amplitude $F^J_{m,m'}$, we must match the right side of (4.1) with ψ at the boundary $r=A$. Since J is a good quantum number, let us first project the Jth partial wave from (4.1). We obtain a set of equations

$$\psi^J_m=\tfrac{1}{2}e^{-im\alpha}i^{J-m}H^{(2)}_{J-m}(k_mA)+\tfrac{1}{2}\sum_{m'}H^{(1)}_{J-m'}(k_{m'}A)i^{J-m'}e^{-im'\alpha}S^J_{m',m} \ , \quad (4.7)$$

where ψ^J_m is the Jth partial wave of (2.11). From (4.7) we can project out the m'th rotational state, which is designated by

$$\langle m' \mid \psi_m \rangle=\frac{1}{\sqrt{2\pi}}\int_0^{2\pi} d\alpha\, e^{im'\alpha}\psi_m(\alpha,A) \ , \quad (4.8)$$

where the index for the total angular momentum (J) have been omitted.

In general, the solution ψ_m will not match the right side of (4.7). Therefore we make a linear combination of ψ_m in such a way that the wave function, and its deriative, is continuous at the boundary $r=A$. In the matrix form, such a linear combination is

$$2\langle \mid \psi\rangle U=i^{J-M}H^{(2)}_{J-M}(k_MA)+i^{J-M}H^{(1)}_{J-M}(k_MA)S \quad (4.9)$$

and

$$2\langle \mid \psi'\rangle U=i^{J-M}\frac{d}{dr}H^{(2)}_{J-M}+i^{J-M}\frac{d}{dr}H^{(1)}_{J-M}S \ , \quad (4.10)$$

where M is a diagonal matrix with the elements $M_{m,m}=m$. The matrix U is a linear transformation. If we replace ψ in (4.9) and (4.10) by $r^{-1/2}\psi$ then the S matrix is obtained

$$S=i^M H^{(1)-1}_{J-M}(k_MA)[k_M\bar{H}^{(1)}_{J-M}H^{(1)-1}_{J-M}+\frac{1}{2A}-\langle \mid \psi'\rangle\langle \mid \psi\rangle^{-1}]^{-1} \times\left[\langle \mid \psi'\rangle\langle \mid \psi\rangle^{-1}-\frac{1}{2A}-k_M\bar{H}^{(2)}_{J-M}H^{(2)-1}_{J-M}\right]i^{-M}H^{(2)}_{J-M}(k_MA) \ , \quad (4.11)$$

where the overbar above the Hankel functions designates the derivative with respect to k_MA.

In the expression for the S matrix (4.11), we still have to evaluate the projection of the m'th rotational state from ψ_m, given by (4.8). From the definition (2.9) of χ^p_m and the expansion (2.11), the projection is

$$\langle m' \mid \psi^p_m \rangle = \frac{1}{\sqrt{2\pi}} \sum_\mu \int_0^{2\pi} d\alpha\, e^{im'\alpha} \chi^p_\mu \varphi^p_{\mu,m} = \sum_\mu \Omega^p_{m',\mu} \varphi^p_{\mu,m} \tag{4.12}$$

or in the matrix notation

$$\langle \mid \psi^p \rangle = \Omega^p \varphi^p \,, \tag{4.13}$$

where the parity p is again introduced, defined in Sec. II. The matrix elements of Ω^p can be calculated, and they are

$$\Omega^p_{m,m} = i \frac{\sqrt{2}}{\pi} \frac{n}{(a+m)^2 - n^2} e^{i(\pi/2)(a+n-m)} \sin\left[\frac{\pi}{2}(a+n-m)[1+p(-1)^m]\right] , \tag{4.14}$$

where $a = -J/(1+\epsilon A^2)$. Since Ω^p is a transformation between the orthonormal sets

$$\Omega^p \Omega^{p+} = I \,. \tag{4.15}$$

At this point it is worth making a comment about (4.11) and (4.14). We have implicitly assumed that the expansion of the wave function is in the basis (2.9). However, in Sec. III. we obtained the radial equations for φ in the basis (2.12) and later the function y, defined by the transformations (3.5) and (3.6). Therefore, we have to find the connection between the S matrix (4.11) and the function y_R.

If we take the inverse of (3.5) and assume the limit $r \to A$, we obtain

$$y^{-1} = T^+ \varphi_0' \varphi_0^{-1} T - \frac{2\alpha_0'}{\pi} T^+ E T \,, \tag{4.16}$$

where φ_0 is the radial equation corresponding to the basis χ_0. The radial solution φ_0 is related to φ, the radial solution in the basis χ, by

$$\varphi_0 = T\varphi \,, \tag{4.17}$$

hence (4.16) is

$$y^{-1} = T^+ T' + \varphi' \varphi^{-1} - \frac{2\alpha_0'}{\pi} T^+ E T \,. \tag{4.18}$$

We can easily prove that $E = \langle \chi_0 \mid \chi_0' \rangle$ and $T = \langle \chi_0 \mid \chi \rangle$ in which case

$$y^{-1} = \varphi' \varphi^{-1} + \langle \chi \mid \chi' \rangle + \langle \chi \mid \chi_0 \rangle \langle \chi_0' \mid \chi \rangle + \langle \chi \mid \chi_0 \rangle \langle \chi_0 \mid \chi_0' \rangle \langle \chi_0 \mid \chi \rangle \,, \tag{4.19}$$

and from the unitarity of T, we find

$$y^{-1} = \varphi' \varphi^{-1} - \langle \chi' \mid \chi \rangle \,. \tag{4.20}$$

On the other hand, the matrix $\langle \mid \psi^{p'} \rangle \langle \mid \psi^p \rangle^{-1}$, which enters (4.11), is

$$\langle \mid \psi^{p'} \rangle \langle \mid \psi^p \rangle^{-1} = \Omega^{p'} \Omega^{p+} + \Omega^p \varphi' \varphi^{-1} \Omega^{p+} \,, \tag{4.21}$$

where we have used

$$\langle \mid \psi^{p'} \rangle = \Omega^{p'} \varphi + \Omega^p \varphi' \tag{4.22}$$

obtained from (4.13). Replacing $\varphi' \varphi^{-1}$ in (4.21) by (4.20), the final form for (4.21) is

$$\langle \mid \psi^{p'} \rangle \langle \mid \psi^p \rangle^{-1} = \Omega^p y^{-1} \Omega^{p+} \,. \tag{4.23}$$

In the derivation of (4.23) we have also used the completeness relation for χ_0 and

$$\Omega^{p'} \Omega^{p+} + \Omega^p \Omega^{p+'} = 0 \tag{4.24}$$

obtained from (4.15).

Therefore, we have proved that the S matrix is related to y^{-1}, through the transformation (4.23). It can be shown, if we define a real Ω^p by

$$\Omega^p_{m,n} = \frac{\sqrt{2}}{\pi} \frac{n}{(a+m)^2 - n^2} \sin\left[\frac{\pi}{2}(a+n-m)\right] \cos\left[\pi \,\mathrm{Int}\left[\frac{n+1}{2}\right]\right] [1+p(-1)^m] \,, \tag{4.25}$$

(where Int represents the integer part of a number) that the S matrix is

$$S = -j^{-1} j^* \,, \tag{4.26}$$

where the Jost function is

$$j = [\Omega^p y_R \tilde{\Omega}^p - k_M^{-1} h^{(1)}_{J-M} (\bar{h}^{(1)}_{J-M})^{-1}] k_M^{1/2} \bar{h}^{(1)}_{J-M} \tag{4.27}$$

with the definition $h^{(1)}_{J-M} = (k_M A)^{1/2} H^{(1)}_{J-M}(k_M A)$.

Let us briefly discuss Ω^p. The first index is the rotational quantum number, while the second takes on positive integer values. Therefore, the matrix Ω^p transforms the indices of the basis set χ into the observable states. The parity p determines which matrix elements of Ω^p are zero, i.e., which rotational states are not present for a given parity. From (4.14) we notice if the parity is positive that all the odd rotational states are missing. Likewise, for the negative parity, all the even rotational states are missing. It follows that the S matrix is a block matrix with no transitions between the states of different parity. In other words, we can formulate the law of conservation of parity, and as a consequence of this law only the even-even/odd-odd transitions are allowed.

There is another interesting property of Ω^p. Since the set of equations for φ is invariant to the parity p, it follows that both even-even and odd-odd transitions are determined by the same solution φ. In other words, the matrix Ω^p makes two different "mixtures" of the same quantity: In one case we obtain even-even and in the other case, odd-odd transitions.

V. DISCUSSION OF y_R

In Sec. III we have given a set of nonlinear equations (3.13) which solve the problem of inelastic collisions of a particle on an ellipsoid. The appropriate S matrix is then given by (4.26). Let us now discuss y. For simplicity we shall suppress the index R in the equations.

The properties of y are determined by the quantities η and λ. In the matrix η there are two terms: one coupling the odd-odd/even-even indices and the other which couples the odd-even. A typical behavior of the matrix elements $\eta_{m,n}$, which couple odd-even indices, is shown in Fig. 3(a) by a broken line. It is finite everywhere, being zero for $r=B$, and acquiring some finite value for $r=A$. On the other hand, the matrix elements of η, which couple the odd-odd/even-even indices, are infinite at both ends [see Figs. 3(a)].

By taking $r\sim B$ we find

$$\eta\sim\frac{1}{2(r-B)}E\ , \tag{5.1}$$

and for $r\sim A$

$$\eta\sim\frac{1}{\pi}\left[\frac{A}{(A^2-B^2)(A-r)}\right]^{1/2}E\ . \tag{5.2}$$

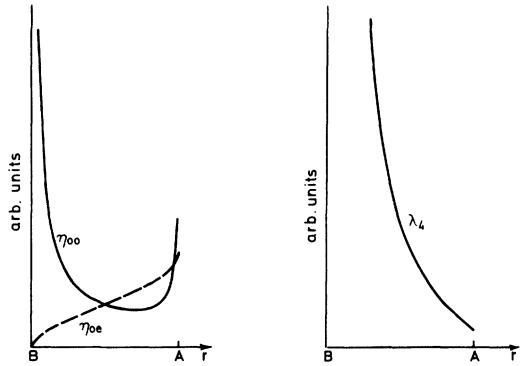

FIG. 3. Plot of typical elements of η and λ. η_{oo} represent elements which couple the odd-odd/even-even indices of y, and η_{oe} those which couple odd-even indices. λ_4 is a typical element of λ for $m=4$.

Although η is infinite at both ends, for $r=A$ the elements show an integrable singularity. In other words, by a simple change of integration variable r to $z=(A-r)^{1/2}$, we obtain a set of equations

$$\frac{dy}{dz}=-2z[I+y\eta-\eta y-y(\lambda-k^2)y]\ , \tag{5.3}$$

where the coefficients are all finite for $z\to 0$, hence the system of equations is integrable at $r=A$.

At the opposite end, i.e, for $r=B$, the solution y can be represented in a power series

$$y=\Delta+\gamma\Delta^2+\cdots\ ,\quad \Delta=r-B \tag{5.4}$$

and if we notice that λ_m is also singular

$$\lambda_m\sim\frac{(1+\epsilon B^2)(A^2-B^2)}{8B^3}\frac{m^2\pi^2}{\Delta}=\beta\frac{m^2}{\Delta}\ , \tag{5.5}$$

we obtain an equation for γ

$$\gamma=\tfrac{1}{4}(\gamma E-E\gamma)-\frac{\beta}{2}M^2\ . \tag{5.6}$$

The equation (5.6) can be solved by defining a unitary matrix U which diagonalizes E (since E is antisymmetric the eigenvalues are imaginary). In that case

$$\gamma=U\Gamma U^+\ , \tag{5.7}$$

where

$$\Gamma_{m,n}=-2\beta\frac{[U^+M^2U]_{m,n}}{4+\epsilon_m-\epsilon_n}\ , \tag{5.8}$$

where ϵ_m are the eigenvalues of E.

In the equation (5.6) we can define δ by replacing $\gamma=(\beta/2)\delta$ to obtain a set of equations independent of β. The set of equations for δ is infinite, and can be solved by truncating the order of E. It

turns out that the matrix elements of δ are the largest on the diagonal and all smaller than N^2, where N is the order of the truncated matrix E. Therefore, the series (5.4) will be of little use for

$$\Delta\frac{\beta}{2}N^2>1 \tag{5.9}$$

or

$$N>\frac{4B}{\pi}\left[\frac{B}{\Delta(A^2-B^2)(1+\epsilon B^2)}\right]^{1/2}, \tag{5.10}$$

which also gives a bound for the accuracy of the series (5.4).

When the series (5.4) is no longer accurate, i.e., for the values of m larger than (5.10), we can use another estimate for the diagonal values of y. Let us assume that in such a case the zeroth-order approximation of y is given by

$$y'_{m,m}\sim 1-m^2\frac{\beta}{\Delta}y^2_{m,m}, \tag{5.11}$$

and the solution is[9]

$$y_{m,m}\sim\left[\frac{\Delta}{\beta}\right]^{1/2}\frac{1}{m}. \tag{5.12}$$

Therefore, for large values of m the diagonal y is small. We will show later that the off-diagonal elements of y are also small for large m.

Let us analyze more closely the matrix λ, introduced in (2.10). It is analogous to the channel energy matrix outside the ellipsoid, but is not equal to it. The reason is that we use the basis set (2.9) for describing the angular function of the rotator. In the simplest case for $J=0$ we have at the boundary $r=A$

$$\lambda_m=\frac{1+\epsilon A^2}{A^2}m^2, \tag{5.13}$$

which corresponds to the energy of rotating ellipsoid $E=\epsilon m^2$ if A is very large or if ϵ is very large. However, we always have inequality

$$\frac{1+\epsilon A^2}{A^2}m^2>\epsilon m^2, \tag{5.14}$$

therefore, in principle, there are always fewer open channels in the set of equations (3.13) than there are energetically accessible. This fact is of importance for calculating approximate solutions. For example, when ϵ is very small we can describe a large number of rotational transitions with a relatively few coupled equations (3.13). In addition, for $\epsilon<<1$ we notice that λ is independent of J, since we have

$$\lambda_m=\frac{\epsilon J^2}{1+\epsilon A^2}+\frac{1+\epsilon A^2}{A^2}m^2\sim\epsilon J^2+\frac{m^2}{A^2}. \tag{5.15}$$

Taking into account that in this limit η is also independent of J [see (A20) and (A21)], the solution y is independent of J. All the J dependence of the S matrix is in Ω, and is therefore kinematic in nature since the transformation Ω is independent of the details of the shape of the target. Such a limiting case of y we will call the "static" solution, since $\epsilon=\mu/I<<1$ implies that the target is much heavier than the incoming particle. From physical intuition we would conclude that under such circumstances the incoming particle will not rotate the target.

One of the disadvantages of the set of equations (3.13) is the difficulty of how to formulate a perturbation scheme for solving them. The reason can be explained briefly. Any approximate solution y_0 of (3.13) can be singular at a set of points r. These values of r are also approximate compared to the exact solution y. Simple analysis shows that the correction to approximate solution will be singular at the same approximate points, determined by y_0. Therefore, if the perturbation scheme does not move the singular points at the same time, the series will not converge to the exact solution. Such a condition is difficult to fulfill for the nonlinear equations (3.13). However, there are cases when this problem does not arise. The most obvious case is when the solution is not singular in the interval of integration, $B\le r\le A$. For example, this is the case when the wave vector is small, i.e., for low-energy collisions. This condition is also fulfilled for $A-B<2\pi/k$ or, in some cases, for large J when all the channels are closed or nearly closed.

In all these cases we can proceed as follows. We define a nonperturbed solution

$$(y^{(0)})'=I-(\lambda-k^2)(y^{(0)})^2, \tag{5.16}$$

which is a diagonal matrix. Assuming that η is a perturbation, the first-order correction $y^{(1)}$ is the solution of a linear equation

$$(y^{(1)})'=y^{(0)}\eta-\eta y^{(0)}-y^{(0)}(\lambda-k^2)y^{(1)}-y^{(1)}(\lambda-k^2)y^{(0)}, \tag{5.17}$$

with the solution

$$y^{(1)}_{m,n}=\int_B^r dr'(y^{(0)}_m-y^{(0)}_n)\eta_{m,n}\exp\left[-\int_{r'}^r dr''[y^{(0)}_m(\lambda_m-k^2)+y^{(0)}_n(\lambda_n-k^2)]\right], \tag{5.18}$$

where it was taken into account that $y=0$ for $r\to B$.

We can now discuss y in the limit when both indices m and n of $y_{m,n}$ are large. It was already shown in (5.12) that $y_{m,m}\sim O(1/m)$ and let us now show what the off-diagonal elements look like. If we recall that $y^{(0)}\sim\lambda^{-1/2}$, Eq. (5.18) gives

$$y^{(1)}_{m,n}\sim\int^r dr'(\lambda_n^{-1/2}-\lambda_m^{-1/2})\eta_{m,n}\exp\left[-\int^r dr''(\lambda_m^{1/2}+\lambda_n^{1/2})\right], \tag{5.19}$$

and since $\lambda_m^{1/2}$ is large, most of the contribution to the integral comes from the vicinity of $r'=r$. Therefore, asymptotically we can estimate

$$y^{(1)}_{m,n}\sim O((m+n)^{-2}) . \tag{5.20}$$

In the limit for large m and n the off-diagonal elements of y go to zero faster than the diagonal ones. This fact is important when deciding where to truncate the set of differential equations for y. In general, we notice that at least the open channels should be included in the set of equations for y, because for the closed channels there is the estimate (5.12) and (5.20). From (5.13) we obtain the number of channels required for numerical integration of y:

$$m=kA(1+\epsilon A^2)^{-1/2} . \tag{5.21}$$

For small ϵ this number is considerably smaller than the number of physically open channels, as was discussed in (5.14). However, the estimate (5.21) may not always be true, such as in the case when $A-B\sim 0$. This point will be discussed in Sec. VI.

VI. S MATRIX AND THE CROSS SECTIONS

Having discussed y in Sec. V, let us now turn our attention to the S matrix given by (4.26). It was shown that the S matrix was determined by the Jost function

$$j=[\Omega y\tilde{\Omega}-k_M^{-1}h^{(1)}_{J-M}\bar{h}^{(1)-1}_{J-M}]k_M^{1/2}\bar{h}^{(1)}_{J-M} , \tag{6.1}$$

where the relevant quantities were defined in Sec. V. Since y and Ω are real, and the only complex quantity in the bracket of (6.1) is the diagonal matrix of the ratio of two Hankel functions; the S matrix is a block matrix. It can be shown that the submatrix corresponding to the open channels, i.e., the channels with $k^2-\epsilon m^2>0$, is unitary. The submatrix corresponding to the closed channels, i.e., the channels with $k^2-\epsilon m^2<0$, is a unit matrix, while the submatrix corresponding to the open-closed channels is exactly zero. Therefore, we pay our attention to only the open-channel submatrix.

As we have mentioned, there are $m=k/\sqrt{\epsilon}$ open channels. However, among them there are channels which have very small transition probability, and in the classical limit they are forbidden. Such transitions can be deduced from (6.1). For an arbitrary J we notice that the ratio of the Hankel functions in (6.1) is complex for

$$|J-m|\lesssim A(k^2-\epsilon m^2)^{1/2} , \tag{6.2}$$

otherwise it is almost real. Therefore, the S matrix for the open channels is also a block matrix: one block corresponding to the allowed transitions, with the dimension given by (6.2), and the other which represents the forbidden transitions. The third block, with the mixed indices from the two previous blocks, is almost zero. The estimate (6.2) gives an upper bound for the allowed transitions and is purely kinematic in nature. To explain this, let us notice that the total angular momentum J is conserved. Therefore, if the ellipsoid is in the mth rotational state the maximum possible orbital angular momentum can be $l_{\max}=A(k^2-\epsilon m^2)^{1/2}$, and their sum must be J, which is exactly the condition (6.2).

We can obtain the maximum kinematic bound for the allowed transitions. Let us first notice that all the allowed transitions are observed for $\theta=180°$. In Sec. VII we will show how to calculate the approximate deflection function for the transition $m_0\to m$. From there we can deduce that for $J=mk/[k+(k^2-\epsilon m^2)^{1/2}]$ and $m_0=0$, the deflection angle is $\theta=180°$. Therefore, if J in (6.2) is replaced by this value, we find

$$m/[k+(k^2-\epsilon m^2)^{1/2}]<A , \tag{6.3}$$

and one can show that this bound is always greater than the dynamic bound[1]

$$m\le 2k(A-B)/[1+\epsilon(A-B)^2] . \tag{6.4}$$

Therefore, the kinematical forbidden transitions have no consequence on the rotational transitions.

Let us now look at a particular example of nearly elastic collisions, i.e., the most dominant mode of scattering is the elastic channel. Such a case is usually referred to as the weak-coupling limit. Physically, this will occur if $A \sim B$, i.e., the target is almost a sphere. However, $A \sim B$ does not imply a small number of inelastic channels, since the scattering energy should also be taken into account. To determine the proper condition of validity for the weak-coupling limit, we can use (6.4). It was mentioned that the weak-coupling limit is applicable for the case when there are few inelastic channels. In the simplest case of one allowed transition $0 \rightarrow 2$, the limit (6.4) gives

$$\Delta = A - B = \frac{k - (k^2 - 4\epsilon)^{1/2}}{2\epsilon} \lesssim \frac{1}{k} , \tag{6.5}$$

where in the last step we have assumed that ϵ is smaller than k^2. Therefore, the weak-coupling limit is applicable to the cases when $\Delta = A - B$ is equal to or smaller than the wavelength of the incoming particle, having the reduced mass of the system.

If the condition (6.5) is fulfilled, then y is approximately (5.4), hence small. In such a case, the S matrix is

$$S \sim h^{(2)}_{J-M} h^{(1)-1}_{J-M} + \frac{4i}{\pi} k_M^{1/2} h^{(1)-1}_{J-M} \Omega y \tilde{\Omega} k_M^{1/2} h^{(1)-1}_{J-M} . \tag{6.6}$$

However, things are not that simple. If we recall from Sec. V that γ, given by (5.7), has diagonal elements of the order m^2 (the off-diagonal elements are smaller) and that the matrix elements of Ω are of the order $\Omega_{m,k} \sim O(k^{-1})$, it is easily deduced that the sum $\Omega y \tilde{\Omega}$ is not convergent. However, for m larger than (5.10), the elements of y are no longer given by (5.4) but are proportional to m^{-1}. Therefore, the sum in $\Omega y \tilde{\Omega}$ stops at $m = N$, where N is given by (5.10). This is, at the same time, the number of basis functions required to achieve convergence in y. For $A \sim B$ in (5.10) we obtain

$$N \sim 4B / \{ \pi \Delta [2(1 + \epsilon A^2)]^{1/2} \} , \tag{6.7}$$

which gives the impossible result that for $A - B \rightarrow 0$, we require an infinite number of equations for a good description of the S matrix. If we compare the estimate of convergence (6.7) with the estimate (5.21), we notice that for a certain value of Δ, the estimate (5.21) is no longer valid. We easily find that the turning point at which this happens is

$$\Delta \lesssim 1/k , \tag{6.8}$$

which is also the condition for the weak-coupling limit.

The reason why the method fails for the weak-coupling limit is understandable (it actually does not fail but becomes inconvenient). If we analyze the way the problem of atom ellipsoid is solved, it is essentially the adiabatic method. It is well known[11] that such a method is complementary to the weak-coupling limit (sometimes the former is also referred to as the strong-coupling limit). In other words, the strong-coupling theory replaces the weak-coupling theory, when the latter fails and vice versa. Therefore, the method suggested in this work is not expected to be convenient in the weak-coupling limit. Another qualitative explanation why the weak-coupling limit is so inconvenient in our model will be given in Sec. IX.

A few typical examples were calculated to illustrate the theory. In our calculations we neglected the odd-even coupling elements in the matrix η. When they are included, the cross sections do not change significantly.

Figure 4 shows the differential cross section for $A = 2$, $B = 1.9$, $\epsilon = 1$, and energy $k^2 = 200A^{-2}$. This is an example of the weak-coupling limit since the inelastic cross section is much smaller than the elastic one. It should be pointed out that at this energy there are up to $m = 14$ open channels, however, from (6.3) we find that only the

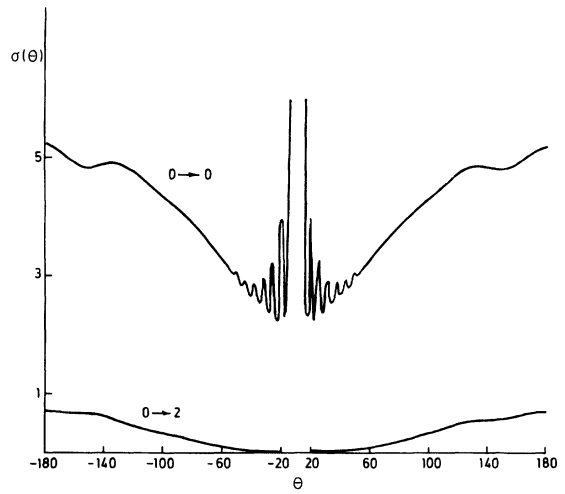

FIG. 4. Cross sections for $A = 2$, $B = 1.9$, $\epsilon = 1$, $k^2 = 200A^{-2}$. The elastic differential cross section is symmetric with respect to $\theta \rightarrow -\theta$. The fast oscillations in the $0 \rightarrow 0$ transition are due to diffraction scattering.

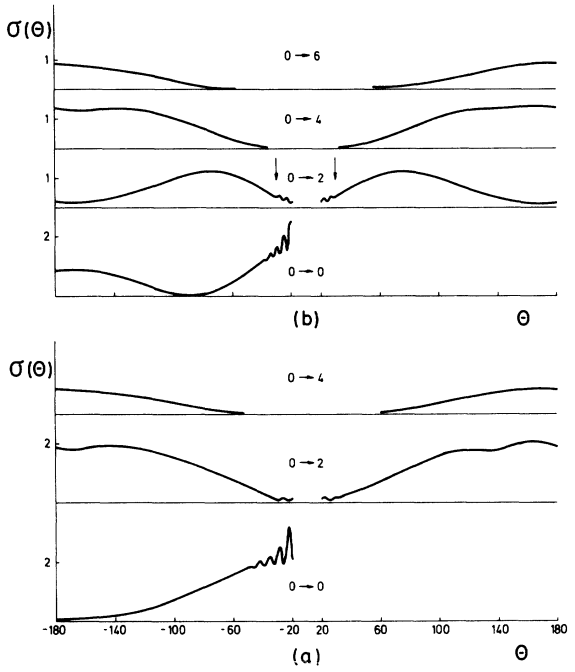

FIG. 5. (a) Cross sections for $A=2$, $B=1.8$, $\epsilon=1$, and $k^2=200A^{-2}$. (b) Cross sections for $A=2$, $B=1.8$, $\epsilon=2$, and $k^2=400A^{-2}$. In both graphs the elastic cross section for $\theta>0$ is not shown because it is mirror image of $\theta<0$.

$0\rightarrow 2$ transition is allowed. The calculation indeed shows that $0\rightarrow 4$ is negligible. As expected from the classical calculation,[1] the inelastic cross section is small in the forward direction, which is also clearly shown in Fig. 4.

By taking different parameters: $A=2$, $B=1.8$, $\epsilon=1$, and $k^2=200A^{-2}$, the inelastic channels become significant, as shown in Fig. 5(a). The pattern of the cross sections changes and becomes more complicated. For these parameters, the maximum classically allowed transition is $0\rightarrow 4$, while the number of open channels is as before, i.e., $m=14$. If the energy is increased to $k^2=400A^{-2}$ and for $\epsilon=2$ (for these parameters there are $m=14$ open channels and the transition $0\rightarrow 6$ in maximally allowed), the picture changes further, as shown in Fig. 5(b). The elastic cross section oscillates while the inelastic $0\rightarrow 2$ transition shows a clear maximum. The position of the maximum is predicted in the classical model and is indicated by an arrow. The agreement is not very good but one can argue that since the position is determined from the classical model, and this is quantum calculation, there should be some discrepancy. The source of oscillations will be discussed in Sec. VII.

If the difference $A-B$ is increased by taking the parameters $A=2$, $B=1.5$, $\epsilon=1$, and $k^2=200A^{-2}$, the maximum classically allowed transition is $0\rightarrow 10$. In Fig. 6 the cross sections are shown for all transitions, including one classically forbidden ($0\rightarrow 12$). Again the arrows indicate the classical positions of the first maxima in the forward direction. We may notice further increase in the complexity of the cross section.

Finally, let us discuss the ϵ dependence of the cross section. In many physical cases ϵ is small, therefore there is a large number of open channels. However, as we have already pointed out, only a small part of them is actually accessible in a transition from the state $m=0$. The classical model gives for the maximum transition $0\rightarrow m_{\max}=2k(A-B)/[1+\epsilon(A-B)^2]$, which is indeed a small fraction of $m=k/\sqrt{\epsilon}$, the number of open channels. In fact, if $\epsilon=0$, there is an infinite number of open channels but there are only $m_{\max}=2k(A-B)$ accessible, or classically allowed, transitions from $m=0$. Let is now assume that ϵ is small but not equal to zero. The number of accessible states will decrease, compared with the case $\epsilon=0$. We expect that if this decrease is not greater than $\Delta m=2$, the differential cross section does not change appreciably. To support this, let us first notice that since $\Delta m=2$ is the minimum quantum of transition, the difference $A-B$ is undetermined by an amount[1] $\delta(A-B)\sim\hbar/k$. Therefore, the argument also applies to ϵ but we will put it the other way around: What variation in ϵ causes the change in the allowed transitions smaller than $\Delta m=2$? Within this variation of ϵ there will be no apparent change in the cross section. To answer the question, and assuming that initially $\epsilon=0$, we must solve the equation

$$2=2k(A-B)-\frac{2k(A-B)}{1+\epsilon(A-B)^2}\ . \tag{6.9}$$

The solution is

$$\epsilon=\frac{1}{\Delta^2(k\Delta-1)},\quad \Delta=A-B\ . \tag{6.10}$$

This result can be used in practice. For example, if for a certain system ϵ is very small, the minimum number of equations one has to solve to obtain the cross sections is $n\sim Ak$. However, with the value of ϵ, given by (6.10), this number is $n\sim Ak/(1+\epsilon A^2)^{1/2}$, which can be much smaller than $n\sim Ak$. At the same time we are sure that the cross sections will not be appreciably different for the two values of ϵ. The test calculation was

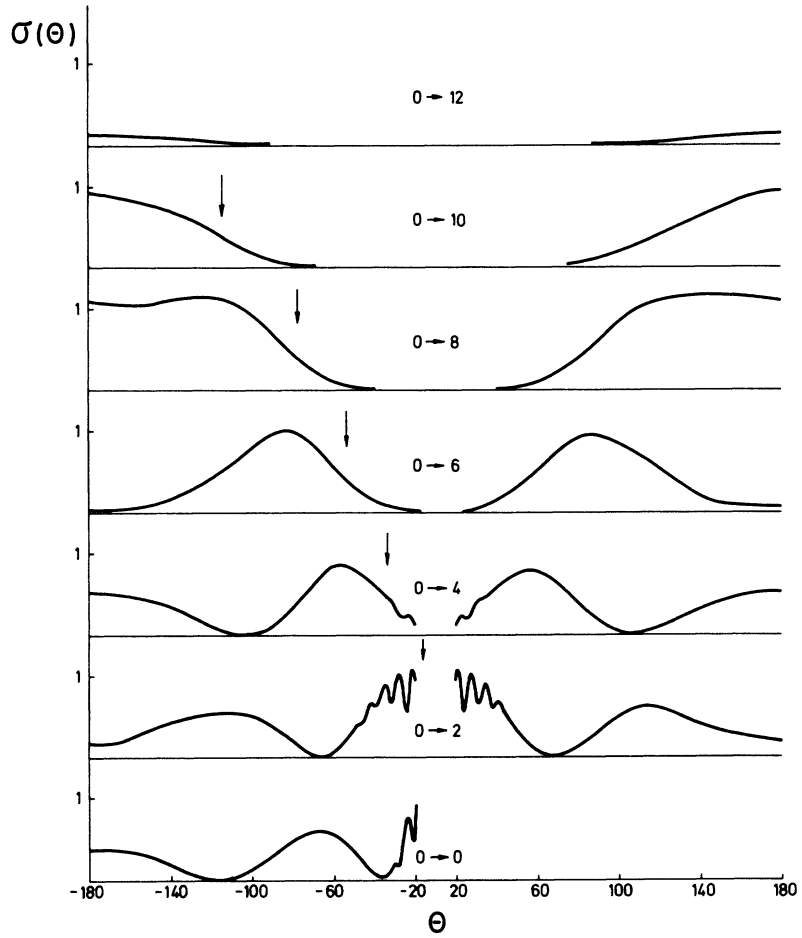

FIG. 6. Cross sections for $A=2$, $B=1.5$, $\epsilon=1$, and $k^2=200A^{-2}$. The transition $0\rightarrow 12$ is classically forbidden. However, due to the uncertainty principle we observe small contribution. The arrows indicate the position of the classical position of the rotational rainbow.

performed for the parameters $A=3.975$, $B=3.286$, $\epsilon=0.03375$, and $k^2=177.4A^{-2}$, which are the parameters for the $He-Na_2$ system.[12] The minimum number of equations, per partial wave, is $n=42$. The number of open channels is $m_{\text{open}}=72$, and the maximum accessible rotational state is $m_{\max}=18$. However, by changing ϵ to $\epsilon=0.2$, the maximum accessible state becomes $m_{\max}=16$, but the number of equations is $n=25$.

Calculations for both parameters are presented in Fig. 7. and the difference in the cross sections between the two values is approximately the thickness of the solid line. Calculation with the value $\epsilon=1$ is also shown in the same figure with the crosses. For the transitions up to $0\rightarrow 6$, the change is not drastic; however, for larger transitions the deviation is very apparent.

VII. SEMICLASSICAL LIMIT

In the analysis of the inelastic collisions it is important to have a tool which offers a simple explanation of the features of the cross sections. In Sec. VI we have shown a few examples of the cross sections which need explanation. In fact, we would like to make a similar analysis to Ford and Wheeler's work[13] for a single-channel case, but generalized to multichannel processes. Formally speaking, this is achieved by taking the limit $\hbar\rightarrow 0$ in the Scrhödinger equation and then analyzing the solution in terms of some classical phenomena.

There are two approaches to obtain the semiclassical limit: (a) the Feynman method of path integrals,[14–16] and (b) the asymptotic solution of differential equations.[17–20] For our purpose we will

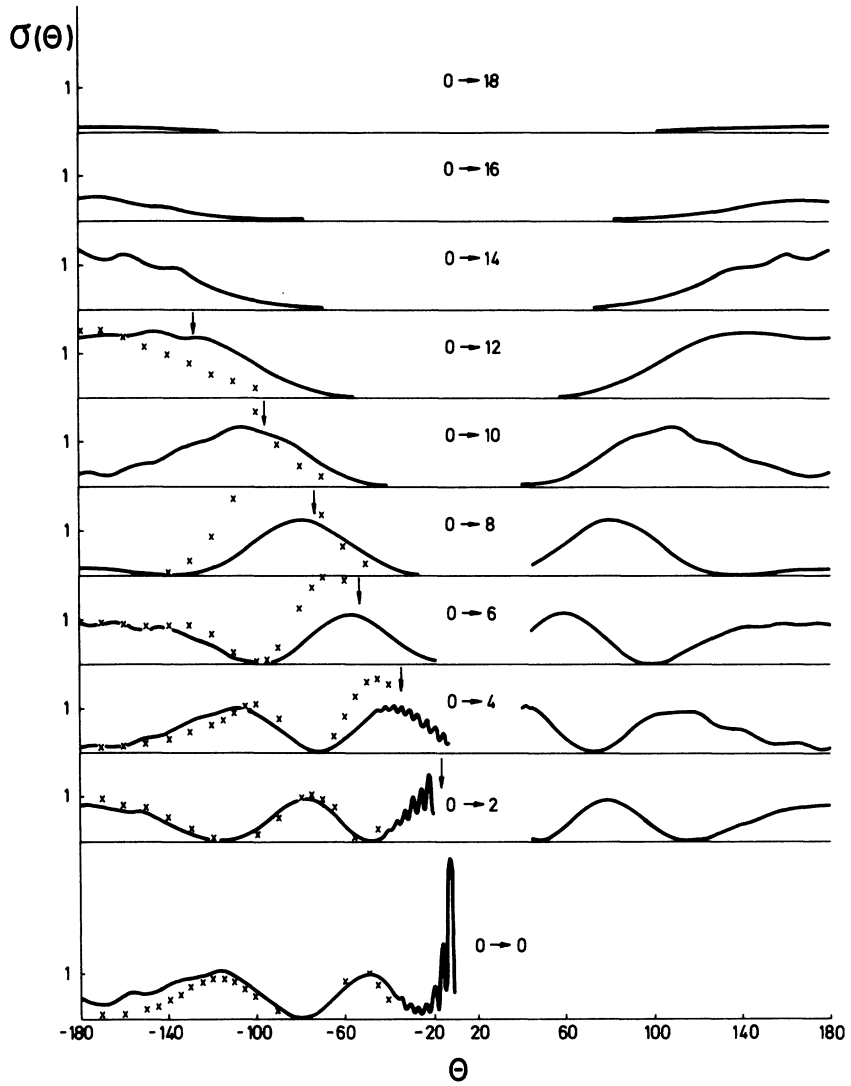

FIG. 7. Cross sections for $A=3.975$, $B=3.286$, $\epsilon=0.033\,75$, and $k^2=177.4A^{-2}$. The parameters describe the $He-Na_2$ system at this energy. The cross sections for $\epsilon=1$ are shown by the crosses. The arrows indicate the classical position of the rotational rainbow.

use both methods but the emphasis is on the asymptotic solution since we work with multichannel equations.

As we have already mentioned, the semiclassical limit is obtained by taking $\hbar\to 0$. Among the schemes to obtain this limit is also a semiclassical perturbation method,[11] which is in the first order of perturbation gives very good results. In this method we can take the limit $\hbar\to 0$, therefore it would appear that it is suitable for analyzing the rotationally inelastic collisions. However, this is not so because in the semiclassical perturbation method we make an important assumption: The coupling matrix η,[11] which is defined in the same way as η_R in (3.13), must not depend on $\hbar$. In rotationally inelastic collisions this assumption is not valid. Let us briefly explain the reason why. The channel energy of the rotor is $k_m^2=k^2-\epsilon m^2$, and we notice that in the limit $\hbar\to 0$, the number of open channels increases as $\hbar^{-1}$ (the wave number k increases as $\hbar^{-1}$ and ϵ is $\hbar$ independent). Therefore, the number of equations in (3.13) also increases as $\hbar^{-1}$ which is obvious from the relationship (5.21). This would not be a big obstacle if the matrix η is not dependent on $\hbar$. However, for the rotational excitations, the η matrix is proportional to the E matrix, defined in (3.4a). It is easily shown that the coupling between two neighboring

channels m and $m+2$ is proportional to m. Hence the η matrix depends on $\hbar$ as $\eta \sim \hbar^{-1}$.

Let us look at a particular case when some information on the semiclassical limit can be obtained. The inelastic S-matrix elements are "sandwiched" between two Hankel functions

$$S^J_{m_0,m} = (\bar{h}^{(1)}_{J-m_0})^{-1} T^J_{m_0,m} \bar{h}^{(2)}_{J-m} , \tag{7.1}$$

where $T^J_{m_0,m}$ is the ratio of two matrices defined by (4.27). In some cases, the function $T^J_{m_0,m}$ is slowly varying with J, e.g., the weak-coupling limit. The variation of the phase of the S-matrix elements is, therefore, entirely determined by the phase of the Hankel functions. Hence

$$\arg(S_{m_0,m})^J = \arg[H^{(2)}_{J-m}(k_m A)] - \arg[H^{(1)}_{J-m_0}(k_{m_0} A)] . \tag{7.2}$$

and if one assumes that the argument of the Hankel functions is much larger than the order, we can write[21]

$$\arg[H^{(1)}_{J-m_0}(k_{m_0}A)] \sim i[A^2 k^2_{m_0} - (J-m_0)^2]^{1/2} - (J-m_0) \ln \frac{J-m_0 + i[A^2 k^2_{m_0} - (J-m_0)^2]^{1/2}}{A k_{m_0}} . \tag{7.3}$$

In analogy with the elastic collisions, we can now associate the derivative $\partial \arg(S^J_{m_0,m})/\partial J$ with the scattering angle $\theta_{m_0,m}$ for this transition. Taking into account (7.2) and (7.3), we find

$$\theta_{m_0,m} = \cos^{-1} \frac{J-m_0}{A k_{m_0}} + \cos^{-1} \frac{J-m}{A k_m} . \tag{7.4}$$

For small J and $m_0 = 0$, the expression (7.4) simplifies and is

$$\theta_{0,m} \sim \pi - \frac{2J-m}{Ak} , \tag{7.5}$$

which is exactly the scattering angle in the classical model[1]

$$\theta^{cl}_{0,m} \sim \pi - \frac{2}{A}\left[b - \frac{m}{2k} \right] \tag{7.6}$$

if the largest parameter b is replaced by J/k. $\theta^{cl}_{0,m}$ was derived under the same assumptions as $\theta_{0,m}$ in (7.5).

Therefore, in the weak-coupling limit we have obtained a partial semiclassical solution of our problem. There still remains the problem to calculate $T^J_{m_0,m}$ but under certain assumptions, discussed in Sec. VI, this can be done within some perturbation scheme. Otherwise one has to solve (3.13) numerically.

Strictly speaking, there are two deflection functions, as discussed for the classical model,[1] each corresponding to a different orientation of the ellipsoid relative to the incoming particle. Since in solving the Schrödinger equation we have taken out this coordinate and replaced it by the potential matrix, we have lost all the information about the correlation between the deflection angle and the orientation angle of the ellipsoid. Hence, the exact deflection function in our calculation will be some average of these in the classical model. Under very special circumstances, these two coincide, as shown earlier. This can be explained most elegantly through the use of the Feynman path integrals. Let the phases and the normalization for the two trajectories be (δ_1, δ_2) and (N_1, N_2), respectively. Then the S matrix is

$$S^J_{m_0,m} = N_1^{-1/2} e^{i\delta_1} + N_2^{-1/2} e^{i\delta_2} , \tag{7.7}$$

which must be compared with (7.1). We find the relationships

$$|S^J_{m_0,m}|^2 = N_1^{-1} + N_2^{-1} + 2(N_1 N_2)^{-1/2} \cos(\delta_2 - \delta_1) \tag{7.8}$$

and

$$\arg(S^J_{m_0,m}) = \tan^{-1} \frac{N_1^{-1/2} \sin\delta_1 + N_2^{-1/2} \sin\delta_2}{N_1^{-1/2} \cos\delta_1 + N_2^{-1/2} \cos\delta_2} . \tag{7.9}$$

The normalization constants are slowly varying functions of J, because they are essentially given by the Jacobian, which only depends on the canonical properties of the coordinates. Furthermore, the numerical calculations show that for some values of J, the modulus of $S^J_{m_0,m}$ is small, almost zero. It can be shown that this is only possible if $N_1 \sim N_2$. Hence, we can write for (7.8)

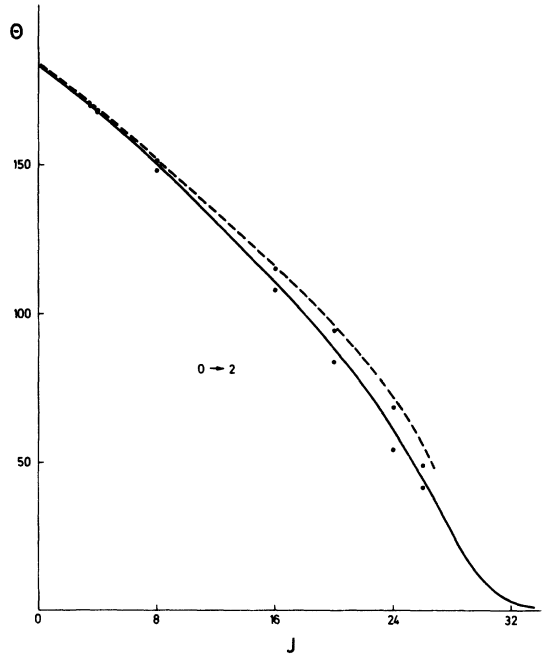

FIG. 8. Deflection functions for the transition $0\rightarrow 2$ in the system from Fig. 5(a). The exact deflection function (——) is an average of the two classical (○). The approximate deflection function (----) of the S matrix in the weak-coupling limit is a very good approximation of the upper classical deflection function.

$$|S^J_{m_0,m}|^2 \sim 4N^2 \cos^2 \frac{\delta_2-\delta_1}{2} . \tag{7.10}$$

The deflection function can also be obtained. Assuming $(N_1/N_2)^{1/2}=x=1+\nu$, where ν is small, we obtain

$$\theta_{m_0,m} \sim \frac{\theta^{(1)}_{m_0,m}+\theta^{(2)}_{m_0,m}}{2} + \frac{\nu}{4\cos^2\frac{\delta_2-\delta_1}{2}}(\theta^{(2)}_{m_0,m}-\theta^{(1)}_{m_0,m})+O(\nu^2) , \tag{7.11}$$

where $\theta^{(1)}_{m_0,m}$ and $\theta^{(1)}_{m_0,m}$ are the classical deflection functions. In the derivation of (7.11) it was assumed that $|\cos(\delta_2-\delta_1)/2| >> \nu$. For $\cos(\delta_2-\delta_1)/2\sim 0$, we find another form of $\theta_{m_0,m}$:

$$\theta_{m_0,m} \sim \frac{\theta^{(2)}_{m_0,m}-\theta^{(1)}_{m_0,m}}{\nu} . \tag{7.12}$$

Therefore, whenever the modulus of the S-matrix element goes through the minimum, the deflection function undergoes rapid change. In all other cases, the deflection function is nearly an average of the two classical funtions, as shown by (7.11).

To illustrate the theory we have calculated three examples of deflection functions. In Fig. 8 the parameters are $A=2$, $B=1.8$, $\epsilon=1$, and $k^2=200A^{-2}$, and the deflection function is for $0\rightarrow 2$. The circles indicate a few points of the two classical deflection functions. The broken line is the deflection function (7.4), which is a very good approximation to the upper classical deflection function. The full line is the true deflection function from our calculations.

In Figs. 9(a) and 9(b) we show that the deflection functions for an ellipsoid with the parameters $A=2$, $B=1.5$, $\epsilon=1$, and $k^2=200A^{-2}$, for the transitions $0\rightarrow 2$ and $0\rightarrow 6$, respectively. Again the broken line represents the deflection function (7.4), which is also a good approximation to the upper classical deflection function (circles). The exact deflection function is an average of the classical, except for the singularity near $J=23$ in Fig. 9(a). The source of singularity was explained earlier. The erratic behavior of $\theta_{m_0,m}$ in Fig. 9(b) for $J>25$ is of no importance since in this region the modulus of $S^J_{m_0,m}$ is small.

The approach, which was just described, explains qualitatively the source of broad oscillations in the differential cross sections. They come from the phase difference between the two paths. Physically, this can be seen as the interference of two waves: one scattered from one orientation of the ellipsoid, and the other from the other orientation. The "optical path" difference will cause oscillations in the cross sections.

The semiclassical limit which we have discussed so far still does not answer the basic question: What is the solution of the scattering problem in the limit $\hbar\rightarrow 0$. We have only pointed out some of the difficulties: failure of the standard perturbation techniques for solving coupled equations due to the semiclassical nature of the coupling equations due to the semiclassical nature of the coupling matrix, and then the loss of information about the system if the angular part of the potential is averaged in the angular basis set. Because of the last point we were also unable to analyze the rotational rainbows, which were analyzed within the infinite order sudden (IOS) limit.[22–24] However, in one particular case we can find a closed form for the scattering amplitude, from where we can also obtain the semiclassical limit. This is shown in Sec. VIII.

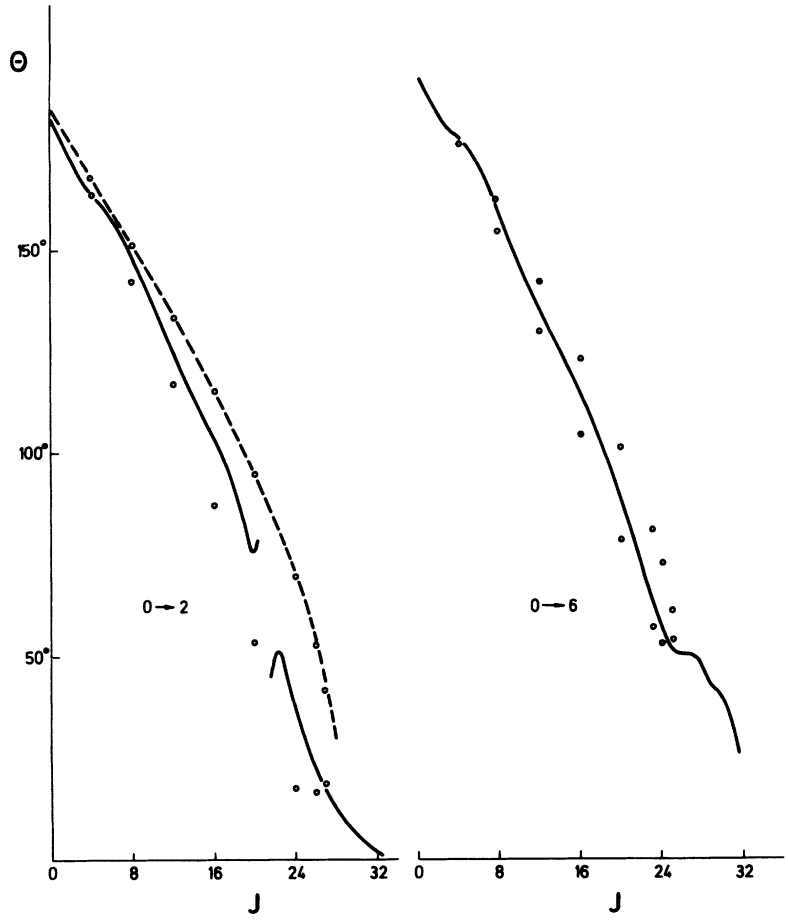

FIG. 9. Deflection function for transition 0→2 and 0→6 of the system from Fig. 7. The exact deflection function (——) follows the approximate formula (7.11) very well. The singularity in the 0→2 deflection function is explained in Eq. (7.12). The circles (○) and the broken line are explained in Fig. 8.

VIII. STATIC SOLUTION

The biggest source of difficulties is incorporated in the use of the cylindrical coordinates. We have pointed out in Sec. II the reason why we use such coordinates for obtaining the multichannel equations. However, we pay the price that the resulting equations are difficult to solve, except numerically. An alternate choice would be the use of the coordinate system appropriate to the topology of the potential. To illustrate this point, let us show that the problem of inelastic scattering on an ellipsoid can be solved in a closed form provided we use a different coordinate system. The problem is solved in the limiting case $\epsilon \to 0$, i.e., the static approximation. This derivation does not imply that for $\epsilon \neq 0$ the solution is also simple. It only shows the relevance of the use of appropriate coordinates in order to obtain a meaningful set of equations.

We have noted in (6.10) that within certain bounds of ϵ, the cross section does not change appreciably. Therefore, for the system for which ϵ is small and less than (6.10), the cross section will not change if we take $\epsilon=0$. Such an approximation we have already named the static approximation, although it is also known as the adiabatic approximation.[25]

Since the topology of the system is entirely determined by the potential, which is the ellipsoid in our case, let us transform the Schrödinger equation into the elliptical coordinates,[7] which are defined as

$$x=\frac{a}{2}ch\rho\cos\beta,\quad y=\frac{a}{2}sh\rho\sin\beta\,,$$
$$a=2(A^2-B^2)^{1/2}\,, \tag{8.1}$$

and (2.1) is

$$\frac{1}{ch^2\rho-\cos^2\beta}\left[\frac{\partial^2\psi}{\partial\rho^2}+\frac{\partial^2\psi}{\partial\beta^2}\right]=-\frac{a}{4}k^2\psi\ . \quad (8.2)$$

The potential is not explicitly given in (8.2) since it is replaced by the boundary condition $\psi=0$ for

$$\rho=\rho_0=\tfrac{1}{2}\ln\frac{A+B}{A-B}\ .$$

A general solution of (8.2) is

$$\psi=\sum_m a_m^e Se_m(\beta)[Je_m(\rho)-Te_m Ne_m(\rho)]+(e\rightarrow o)\ , \quad (8.3)$$

where the symbol $(e\rightarrow o)$ means that in the term preceding it, e, is replaced by o. The periodic Mathieu functions are designated by $Se_m(\beta)$ and $So_m(\beta)$,[26] while the radial Mathieu functions are $Je_m(\rho)$, $Ne_m(\rho)$, $Jo_m(\rho)$, and $No_m(\rho)$. The quantities Te_m and To_m are defined as

$$Te_m=\frac{Je_m(\rho_0)}{Ne_m(\rho_0)},\quad To_m=\frac{Jo_m(\rho_0)}{No_m(\rho_0)}\ . \quad (8.4)$$

The ellipsoid in our problem is fixed so that the major axis is along the x coordinate. The incoming plane wave is

$$\psi_0=e^{ik(x\cos\alpha+y\sin\alpha)} \quad (8.5)$$

which represents the wave traveling at an angle α with respect to the positive x axis. Far away from the fixed ellipse, the scattered wave function is

$$\psi\sim\psi_0+\frac{e^{ikr}}{\sqrt{r}}f(\alpha;\beta)\ , \quad (8.6)$$

where α is the parameter from (8.5). The plane wave (8.5) can be represented in terms of the Mathieu functions[26]

$$\psi_0=\sqrt{8\pi}\sum_m e^{i(\pi/2)m}\frac{Se_m(\alpha)}{M_m^e}Se_m(\beta)Je_m(\rho)+(e\rightarrow o)\ , \quad (8.7)$$

while for the scattering amplitude we write

$$f(\alpha;\beta)=\sum_m f_m^e(\alpha)Se_m(\beta)+(e\rightarrow o)\ . \quad (8.8)$$

Taking the limit $\rho\rightarrow 0$ and equating the coefficients with $\exp(ikr)$ and $\exp(-ikr)$ on both sides of (8.6), we obtain a set of equations for f_m^e and f_m^o. The solution of the equations is

$$f_m^e(\alpha)=\left[\frac{2\pi}{k}\right]^{1/2}e^{-i(\pi/4)}\frac{Se_m(\alpha)}{M_m^e}\left[\frac{i-Te_m}{i+Te_m}-1\right],$$
$$f_m^o(\alpha)=f_m^e(e\rightarrow o)\ , \quad (8.9)$$

and the scattering amplitude is

$$f(\alpha;\beta)=\left[\frac{2\pi}{k}\right]^{1/2}e^{-i(\pi/4)}\sum_m\frac{Se_m(\alpha)}{M_m^e}Se_m(\beta)\left[\frac{i-Te_m}{i+Te_m}-1\right]+(e\rightarrow o)\ . \quad (8.10)$$

Let us now write (8.10) in the form which resembles the inelastic scattering amplitude (4.1). To achieve this, the Mathieu functions in (8.10) are written in the form of expansions in trigonometric functions:

$$Se_m(\alpha)=\tfrac{1}{4}\sum_{n=0}^{\infty}B_n^e(m)(e^{in\alpha}+e^{-in\alpha})(1+(-1)^{m+n})\ ,$$
$$So_m(\alpha)=\frac{1}{4i}\sum_{n=1}^{\infty}B_n^o(m)(e^{in\alpha}-e^{-in\alpha})[1+(-1)^{m+n}]\ . \quad (8.11)$$

Replacing the Mathieu functions in (8.10) with their representation (8.11), the scattering amplitude takes the form

$$f(\alpha;\beta)=\frac{1}{4}\left[\frac{2\pi}{k}\right]^{1/2}e^{-i(\pi/4)}\sum_{\mu,\nu=\text{even}}(e^{i\alpha\nu}+e^{-i\alpha\nu})(e^{i\beta\mu}+e^{-i\beta\mu})F_{\mu,\nu}^e$$
$$-\frac{1}{4}\left[\frac{2\pi}{k}\right]^{1/2}e^{-i(\pi/4)}\sum_{\mu,\nu=\text{even}}(e^{i\alpha\nu}-e^{-i\alpha\nu})(e^{i\beta\mu}-e^{-i\beta\mu})F_{\mu,\nu}^o+(\mu_1\nu=\text{odd})\ , \quad (8.12)$$

where the last term indicates that the summation index takes the odd values. The functions $F_{\mu,\nu}^e$ and $F_{\mu,\nu}^o$ are defined as

$$F^e_{\mu,\nu}=\sum_{m=\text{even}}\frac{B^e_\nu(m)B^e_\mu(m)}{M^e_m}\left[\frac{i-Te_m}{i+Te_m}-1\right],$$
$$F^o_{\mu,\nu}=F^e_{\mu,\nu}(e\to o)\,, \tag{8.13}$$

and similarly for $\mu,\nu=$odd, the summation index m is odd.

The angle α in (8.12) is not the conjugate variable of the rotational quantum number j, and β is not the true scattering angle θ. For $\rho\to\infty$ they are related through the set of equations

$$\phi=-\alpha,\quad \theta=\beta-\alpha\,, \tag{8.14}$$

therefore the scattering amplitude is now

$$f(\phi;\theta)=\frac{1}{4}\left[\frac{2\pi}{k}\right]^{1/2}e^{-i(\pi/4)}\sum_{\mu,\nu=\text{even}}e^{i\mu\theta}[e^{-i\phi(\mu+\nu)}(F^e_{\mu,\nu}-F^o_{\mu,\nu})+e^{i\phi(\nu-\mu)}(F^e_{\mu,\nu}+F^o_{\mu,\nu})]$$
$$+\frac{1}{4}\left[\frac{2\pi}{k}\right]^{1/2}e^{-i(\pi/4)}\sum_{\mu,\nu=\text{even}}e^{-i\mu\theta}[e^{i\phi(\mu+\nu)}(F^e_{\mu,\nu}-F^o_{\mu,\nu})+e^{-i\phi(\nu-\mu)}(F^e_{\mu,\nu}+F^o_{\mu,\nu})]+(\mu,\nu\to\text{odd})\,. \tag{8.15}$$

Let us now associate μ with J and the linear combination of μ and ν in the exponent with j, the rotational quantum number. The first summation in (8.15) therefore goes over the positive and even J and the second goes over the negative and even J. Let us now project out the jth rotational state in (8.15). It is found that the $j=0$ component of $f(\phi;\theta)$ looks like

$$f_0(\theta)=\frac{1}{2}\left[\frac{2\pi}{k}\right]^{1/2}e^{-i(\pi/4)}\left[F^e_{0,0}-F^o_{0,0}+\sum_\mu(F^e_{\mu,\mu}+F^o_{\mu,\mu})\cos\mu\theta\right], \tag{8.16}$$

while for the $j=$even and $j>0$ we have

$$f_j(\theta)=\frac{1}{4}\left[\frac{2\pi}{k}\right]^{1/2}e^{-i(\pi/4)}\left[\sum_{\mu=0}^{\infty}e^{i\mu\theta}(F^e_{\mu,\mu+j}+F^o_{\mu,\mu+j})+\sum_{\mu=0}^{j}e^{-i\mu\theta}(F^e_{\mu,j-\mu}-F^o_{\mu,j-\mu})\right.$$
$$\left.+\sum_{\mu=j}^{\infty}e^{-i\mu\theta}(F_{\mu,\mu-j}+F^o_{\mu,\mu-j})\right]. \tag{8.17}$$

Similarly we obtain $f_j(\theta)$ for $j<0$ and $j=$even:

$$f_j(\theta)=\frac{1}{4}\left[\frac{2\pi}{k}\right]^{1/2}e^{-i(\pi/4)}\left[\sum_{\mu=0}^{\infty}e^{-i\mu\theta}(F^e_{\mu,\mu-j}+F^o_{\mu,\mu-j})+\sum_{\mu=0}^{j}e^{i\mu\theta}(F^e_{\mu,-\mu-j}-F^o_{\mu,-\mu-j})\right.$$
$$\left.+\sum_{\mu=-j}^{\infty}e^{i\mu\theta}(F^e_{\mu,\mu+j}+F^o_{\mu,\mu+j})\right]. \tag{8.18}$$

The projection to any odd j is exactly zero. We can now associate $f_j(\theta)$ with the scattering amplitude for the transitions $0\to j$, since the input channel, given by (8.5), describes the rotor with $j=0$. From the fact that $f_j(\theta)$ for $j=$odd is zero, we have also proved that the $0\to$odd transitions are forbidden.

Generalization to any initial rotation state j_0 is trivial: The incoming wave should have a factor $\exp(ij_0\phi)$ from which it follows that the function $F^e_{\mu,\nu}$ and $F^o_{\mu,\nu}$ should include the factor $\exp(ij_0\phi)$. It can be easily shown that in such a case the scattering amplitude satisfy

$$f_{j_0\to j}(\theta)=f_{0,\to j_0-j}(\theta)\,. \tag{8.19}$$

The derivation of the scattering amplitude in the static limit, and specially the fact that a closed

form was obtained in (8.16)–(8.19), show the relevance of using appropriate coordinates to take into account explicitly the topology of the system. The topology is determined by the hard core of potential. We have shown in the previous sections how this problem was solved in the cylindric coordinates, and found that even in the simple case $\epsilon=0$ the problem could not be solved in a closed form. It should be pointed out that the difficulty with the weak-coupling limit is also partly due to this fact, since the only way to solve the problem in the cylindrical coordinates is to use the adiabatic basis. It does not mean that for $\epsilon\neq 0$ the problem is also easy to solve in the elliptical coordinates. The advantage which we have in the static approximation is that the kinetic energy operator of the rotor is exactly zero, due to $\epsilon=0$, In general, when $\epsilon\neq 0$, the transformation of this operator into the elliptical coordinates is the most complicated part of such an approach.

IX. CONCLUSION

The aim of the present work is to give insight into the nature of inelastic collision processes for rotations. The theory assumed a simple two-dimensional model, in which a particle was scattered by a hard-core ellipsoid.

It would be appropriate to ask what is the relevance of the model to the real potentials. First, the model will certainly not reproduce the features which are due to the details of the potential, such as the attractive part of the potential. The attraction causes two effects: rainbows and resonances (orbiting) which are definitely not observed in our calculations. However, for high-energy scattering such details can be neglected, and the incoming particle only observes the hard core, which determines the topology of the system.

For the real potentials one can also define the weak-coupling limit, when the distorted-wave approximation gives good results. We have shown that within the hard-core ellipsoid model this is not possible. The explanation can be given with qualitative arguments. The weak-coupling limit assumes, among other things $A\sim B$. Let us suppose that for $A>r>B$ we draw a similar picture as in Fig. 2, but for the real potentials. Usually one does not find infinite walls between the regions of zero potential. The smaller the difference $A-B$, the lower the barrier is between these two regions. For a very small $A-B$ the height of the barrier can be negligible in which case the angular wave function of the Hamiltonian will be approximately that of the rigid rotor. Therefore, the diabatic representation, i.e., the representation in which the eigenfunctions of the rigid rotor are $\exp(im\phi)$, will be the most suitable one. It is obvious, if the difference $A-B$ is increased, the diabatic basis goes continuously into the adiabatic.

The property of the diabatic basis is that the eigenfunctions, and their derivatives with respect to ϕ, are continuous for all ϕ. On the other hand, for the hard-core ellipsoid, the eigenfunctions of the right rotor [Eqs. (2.9) and (2.12)] are continuous for all α but their derivative is not, especially in the limit $r\rightarrow A$, where all the functions with the odd indices have noncontinuous derivative at $\alpha=0,\pi$. In the weak-coupling limit, when $r=A$ becomes the point from where most of the contribution to the solution of Schrödinger equation comes, such a set of angular functions becomes inadequate. In fact, the limit $A-B\rightarrow 0$ is not possible since the diabatic set, which is the only set for use in such a case, is not the limit of the adiabatic set χ.

How can the results of the two-dimensional model be generalized to three dimensions? It is obvious that by bringing another degree of freedom, the azimuthal angle, the analytic form of the adiabatic basis is more complicated. It would be much easier to perform the numerical work rather than the analytic. One suggestion is to start from the diabatic basis and calculate the coupling matrix analogous to (2.6). At each point of r the matrix is diagonalized, and as a result we obtain a set of equations in adiabatic basis.[27] Of course, the results should be checked for their independence of the arbitrary factor V_0. A similar procedure can be used for real potentials.

ACKNOWLEDGMENTS

This work was supported in part by the grant from International Büro, KFG Jülich, Federal Republic of Germany. The author wishes to acknowledge the hospitality of Dr. U. Buck at the Max-Planck-Institute für Strömungsforschung in Göttingen, during which stay part of this work was completed.

APPENDIX

Here we will evaluate the matrix $U^{+}U'$, which appears in (3.10), where U is defined in (3.9). Let

us designate this product shortly by η. From the definition of U we obtain

$$\eta = U^+U' = T^+T' - \frac{2\alpha_0'}{\pi - 2\alpha_0} T^+ET \ . \tag{A1}$$

To find the products in (A1), let us recall the definition of T and E. The matrix T is a transformation from the basis set χ^0 to χ, i.e.,

$$|\chi\rangle = T\,|\chi^0\rangle \ , \tag{A2}$$

and is a function of r. E is given by (3.4a) and formally we can write it as a transformation

$$E\,|\chi^0\rangle = -\frac{\pi - 2\alpha_0}{2\alpha_0'}\,|\chi^{0\prime}\rangle \ . \tag{A3}$$

The product T^+T' can now be obtained if we take derivative of (A2) with respect to r:

$$|\chi'\rangle = T'\,|\chi^0\rangle + T\,|\chi_0'\rangle \ , \tag{A4}$$

and after multiplying by T^+ from the left, we have

$$\langle\chi^0|\,T^+\,|\chi'\rangle = \langle\chi^0|\,T^+T'\,|\chi^0\rangle + \langle\chi^0\,|\,\chi^{0\prime}\rangle \ , \tag{A5}$$

where we have taken the matrix element in the basis $|\chi^0\rangle$. Since both sets $|\chi\rangle$ and $|\chi^0\rangle$ form a complete set, we have finally

$$\langle\chi^0|\,T^+T'\,|\chi^0\rangle = \langle\chi\,|\,\chi'\rangle + 2\frac{\alpha_0'}{\pi - 2\alpha_0} E \ , \tag{A6}$$

where we have used (A3). Therefore, the matrix T^+T' in (A1) is proportional to the integral $\langle\chi\,|\,\chi'\rangle$, i.e.,

$$(T^+T')_{m,n} = 2\frac{\alpha_0'}{\pi - 2\alpha_0} E_{m,n} + \int_0^{2\pi} d\alpha\, \chi_m^* \chi_n' \ , \tag{A7}$$

where we have omitted the sign for the parity, since the integral is invariant to it.

From the definition of the basis set χ_m, we obtain

$$\int_0^{2\pi} d\alpha\, \chi_m^* \chi_n' = \frac{\alpha_0'}{\pi - 2\alpha_0}\delta_{m,n} + 2ia' \int_{\alpha_0}^{\pi - \alpha_0} d\alpha\, \alpha \chi_m^* \chi_n + \frac{2n\pi\alpha_0'}{(\pi - 2\alpha_0)^3} \int_{\alpha_0}^{\pi - \alpha_0} d\alpha (2\alpha - \pi) \sin\left[\frac{m\pi}{\pi - 2\alpha_0}(\alpha - \alpha_0)\right] \cos\left[\frac{n\pi}{\pi - 2\alpha_0}(\alpha - \alpha_0)\right] , \tag{A8}$$

which can be integrated analytically, to give

$$(T^+T')_{m,n} = i\frac{\pi a'}{2}\delta_{m,n} + \frac{ia'}{\pi^2}(\pi - 2\alpha_0)\frac{4mn}{(m^2 - n^2)^2}[(-1)^{m+n} - 1] \ , \tag{A9}$$

where

$$a = -\frac{J}{1 + \epsilon r^2} \ . \tag{A10}$$

The product T^+ET can also be obtained in a similar manner. If we notice that $|\chi^0\rangle$ is obtained from $|\chi\rangle$ by a product

$$|\chi^0\rangle = e^{-ia\alpha}\,|\chi\rangle \ , \tag{A11}$$

then after taking derivative of (A1), we have

$$|\chi^{0\prime}\rangle = -ia'\alpha\,|\chi^0\rangle + e^{-ia\alpha}\,|\chi'\rangle = -\frac{2\alpha_0'}{\pi - 2\alpha_0} E\,|\chi^0\rangle \tag{A12}$$

or

$$-\frac{2\alpha_0'}{\pi - 2\alpha_0} E\,|\chi\rangle = |\chi'\rangle - ia'\alpha\,|\chi\rangle \ . \tag{A13}$$

On the other hand, the product T^+ET is in the basis $|\chi^0\rangle$

$$\langle\chi^0|\,T^+ET\,|\chi^0\rangle = \langle\chi\,|\,E\,|\chi\rangle \ , \tag{A14}$$

where we have used the property

$$\langle \chi^0 | T^+ | \chi \rangle = I \tag{A15}$$

and the completeness of $|\chi\rangle$. Hence the matrix (A14) is

$$(T^+ET)_{m,n} = -\frac{\pi - 2\alpha_0}{2\alpha_0'} \left[2 \int_{\alpha_0}^{\pi-\alpha_0} d\alpha \chi_m^+ \chi_n' - 2ia' \int_{\alpha_0}^{\pi-\alpha_0} d\alpha \alpha \chi_m^* \chi_n \right] , \tag{A16}$$

and the η matrix

$$\eta_{m,n} = -\frac{2\alpha_0'}{\pi - 2\alpha_0} E_{m,n} + ia' \frac{\pi}{2} \delta_{m,n} + \frac{ia'}{\pi^2} (\pi - 2\alpha_0) \frac{4mn}{(m^2 - n^2)^2} [(-1)^{m+n} - 1] . \tag{A17}$$

The diagonal term in (A17) is independent of the index, and if we recall that η enters the equation (3.10) as the comutator with y, this term can be neglected. Therefore, we define η as

$$\eta_{m,n} = -\frac{2\alpha_0'}{\pi - 2\alpha_0} E_{m,n} + \frac{ia'}{\pi^2} (\pi - 2\alpha_0) \frac{4mn}{(m^2 - n^2)^2} [(-1)^{m+n} - 1] . \tag{A18}$$

From the structure of (A18) we notice that η is a block matrix: The first term couples only the even-even or odd-odd indices, while the second couples the even-odd indices. We also notice that η is J dependent through the coefficient a, i.e., the total angular momentum J is reponsible for the even-odd coupling in the indices of y.

We also notice that η is complex. However, the matrix elements of the same parity are real, while of the different parity are imaginary. Therefore, we can define a real antisymmetric matrix η_R by the use of transformation defined in (3.11). We can easily show that in such a case

$$\eta = \tfrac{1}{2}(I - iI^-) \eta_R (I - iI^-) , \tag{A19}$$

where η_R is given by (A18) with the imaginary unit i being omitted. In addition, all the terms in the odd-even block matrix, with the property $m < n$, have a minus sign in front, i.e.,

$$(\eta_R)_{m,n} = -\frac{2\alpha_0'}{\pi - 2\alpha_0} E_{m,n} + \frac{a'}{\pi^2} (\pi - 2\alpha_0) \frac{4mn}{(m^2 - n^2)^2} [(-1)^{m+n} - 1] \frac{m - n}{|m - n|} , \tag{A20}$$

where

$$a' = \frac{2\epsilon r J}{(1 + \epsilon r^2)^2} . \tag{A21}$$

[1] S. Bosanac, Phys. Rev. A 22, 2617 (1980).
[2] D. Beck, U. Ross, and W. Schepper, Phys. Rev. A 19, 2173 (1979).
[3] S. Bosanac and U. Buck, Chem. Phys. Lett. 81, 315 (1981).
[4] M. H. Alexander and P. J. Dagdigian, J. Chem. Phys. 73, 1233 (1980).
[5] H. J. Korsch (private communication).
[6] For a review see, D. J. Kouri, *Atom-Molecule Collision Theory,* edited by R. B. Bernstein (Plenum, New York, 1979), Chap. 9.
[7] P. M. Morse and H. Feshbach, *Methods of Theoretical Physics* (McGraw-Hill, New York, 1953), Vol. I, Chap. 5.
[8] M. Born and J. R. Oppenheimer, Ann. Phys. (N.Y.) 84, 457 (1927).
[9] S. Bosanac, Croat. Chem. Acta 49, 471 (1977).
[10] I. S. Gradshteyn and I. M. Ryzhik, *Tables of Integrals, Series and Products* (Academic, London, 1965).
[11] S. Bosanac, J. Math. Phys. 20, 396 (1979).
[12] R. Schinke, W. Müller, W. Meyer, and P. McGuire, J. Chem. Phys. 74, 3916 (1981).
[13] K. W. Ford and J. A. Wheeler, Ann. Phys. (N.Y.) 7, 259 (1959).
[14] R. P. Feynman and A. R. Hibbs, *Quantum Mechanics and Path Integrals* (McGraw-Hill, New York, 1965).
[15] P. Pechukas, Phys. Rev. 181, 166 (1969).
[16] W. H. Miller, Adv. Chem. Phys. 25, 69 (1974).
[17] N. Fröman and P. W. Fröman, *JWKB Approximation* (North-Holland, Amsterdam, 1965).
[18] W. H. Bassichis and A. Dar, Ann. Phys. (N.Y.) 36, 130 (1960).

[19]D. J. Vezzetti and S. I. Rubinow, Ann. Phys. (N.Y.) 35, 373 (1965).
[20]J. B. Delos, W. R. Thorson, and S. K. Knudsen, Phys. Rev. A 6, 709 (1972).
[21]H. M. Nussenzveig, Ann. Phys. (N.Y.) 34, 23 (1965).
[22]R. Schinke, Chem. Phys. 34, 65 (1978).
[23]H. J. Korsch and R. Schinke, J. Chem. Phys. 73, 1222 (1980).
[24]J. M. Bowman, Chem. Phys. Lett. 62, 309 (1979).
[25]S. Drozdov, Zh. Eksp. Teor. Fiz. 28, 734 (1955) [Sov. Phys.—JETP 1, 588 (1955)].
[26]Reference 7, Vol. II, Chap. 11.
[27]The method is in analogy with that of Ref. 11.